ROYAL SOCIETY OF CHEMISTRY

www.rsc.org/dalton

Coordination chemistry of Co complexes containing tridentate SNS ligands and their application as catalysts for the oxidation of n-octane

Lynette Soobramoney,[a] Muhammad D. Bala*[a] and Holger B. Friedrich*[a]

Abstract

The selective oxidation of saturated hydrocarbons to terminal oxygenates under mild catalytic conditions has remained a centuries long challenge to chemical catalysis. In an attempt to address this challenge, two series of tridentate donor ligands {2,6-bis($RSCH_2$)pyridine and bis($RSCH_2CH_2$)amine [R= alkyl, aryl]} and their respective cobalt complexes {Co[2,6-bis($RSCH_2$)pyridine]Cl_2 and Co[bis($RSCH_2CH_2$)amine]Cl_2} have been synthesized and characterized. Crystal structures of Co[2,6-bis($RSCH_2$)pyridine]Cl_2 [R = –CH_3 (**1**), –CH_2CH_3 (**2**), –$CH_2CH_2CH_2CH_3$ (**3**) and –C_6H_5 (**4**)] are reported in which **1** crystallized as a homo-bimetallic dimer that incorporated two bridging chloride atoms in an octahedral geometry around each cobalt center, while **2**, **3** and **4** crystallized as mono-metallic species characterized by trigonal bipyramidal arrangement of ligands around each cobalt center. As catalysts for the homogeneous selective oxidation of *n*-octane, the catalysts yielded ketones as the dominant products with selectivity of ca. 90% for the most active catalyst Co[bis($CH_2CH_2SCH_2CH_2$)amine]Cl_2 (**6**) at a total *n*-octane conversion of 23%. Using *tert*-butyl hydroperoxide (TBHP) as an oxidant, optimization of reaction conditions is also reported.

[a] *School of Chemistry and Physics, University of KwaZulu-Natal, Private Bag X54001, Durban 4000, South Africa*

Address all correspondence to email: bala@ukzn.ac.za (MDB); friedric@ukzn.ac.za (HBF)

Fax: +27 31 260 3091

Introduction

28   Selective activation of paraffins (alkanes) has remained an area of active research interest due

29   to relative inertness of the saturated hydrocarbon bonds. The inertness of paraffins is due to

30   strong, localized C−C and C−H bonds, which makes it difficult for them to participate in

31   chemical reactions. This is because they lack empty orbitals of low energy or filled orbitals of

32   high energy necessary for most chemical transformations.[1, 2] Most attempts at paraffin

33   activation aim to convert the inert alkane to relatively more reactive or value-added products

34   which amongst other uses serve as feedstock, additives or solvents for pharmaceutical and

35   other chemical industries.[3] Oxygenates (alcohols, ketones and carboxylic acids), which result

36   from oxidative functionalization of alkanes, are the most desired products of paraffin activation

37   in chemistry. These are generally believed to be obtained by activation of the C–H bond via

38   bond cleavage, followed by insertion of a single oxygen atom from an appropriate donor to the

39   activated specie.[4]

40   Although a number of researchers have reported on the use of transition metal complexes in the

41   catalytic activation of paraffins,[4-11] the employment of pincer complexes in this regards has

42   remained challenging to scientists worldwide. Hence, there are only a handful of reported

43   examples on the utilization of pincer ligand-based metal complexes for the catalytic activation

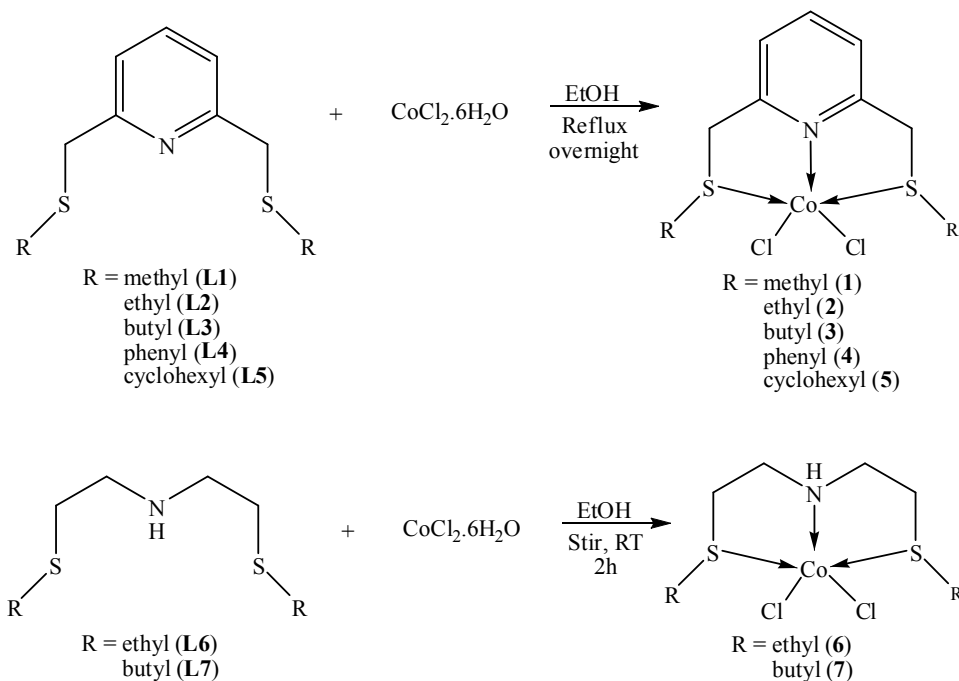44   of *mainly aryl and vinyl C–H bonds*.[2, 12-23]

45   Since their discovery in the mid-1970s, pincer-type ligands have become increasingly

46   important in chemistry,[24] and owing to the ability to tailor the reactivity, selectivity and

47   stability of the ligands towards a specific reaction pathway or product, the application of

48   pincer-based metal complexes has dramatically increased.[18, 25-27] These advantages are due to

49   the terdentate binding mode of the ligands which implies they are able to stabilize metal

50   centers more effectively as compared to related mono or bidentate variants. In addition to

51   imparting stability, simultaneous occupation of multiple coordination sites around a metal

52   center allows the ligands to control access to the center which in turn affects binding of

53   reactive species, thus providing enhanced selectivity towards a desired substrate during

54   catalysis. The ligands are also easily tuned, both electronically and sterically to ensure catalyst

55   versatility.[25,27] It is worth noting that in spite of the increased interest in pincer complexes,

56   those complexes stabilized by ligands typified by SNS donor atom combination have in general

57   received relatively less attention.

58   However, since the discovery of SNS complexes of Cr[28] as an excellent ethylene trimerization

59   catalyst, interest in SNS ligands has also increased amongst researchers. In addition to the

60   seminal report by McGuinness, Wasserscheid and co-workers[28], SNS complexes of Mo,[29] Pt,[30]

61   Pd,[31] Ru,[32] Cu,[33] Ni,[34] and Zn[35] have to date been synthesized and characterized. One of the

62   key features of the SNS pincer ligand relevant to its application in catalysis, is that it may be

63   designed to adopt a hemilabile binding mode.[36] This is usually achieved by exploiting the

64   relative difference in binding abilities between the hard nitrogen donor and the soft sulfur

65   donor atoms to metal centers.[37] Being hemilabile also affords the metal complex with greater

66   flexibility and balance between stability and reactivity.[38, 39]

67   To the best of our knowledge, there has been no work reported on Co-based SNS complexes or

68   the application of SNS pincer complexes for C–H or paraffin activation. Hence this study

69   reports on the first examples of a new range of Co-based SNS pincer complexes and their

70   successful application as catalysts in the activation and functionalization of *n*-octane.

71

72   **Scheme 1: Synthetic route to SNS-Co(II) complexes 1-7**

R = methyl (**L1**)
ethyl (**L2**)
butyl (**L3**)
phenyl (**L4**)
cyclohexyl (**L5**)

R = methyl (**1**)
ethyl (**2**)
butyl (**3**)
phenyl (**4**)
cyclohexyl (**5**)

R = ethyl (**L6**)
butyl (**L7**)

R = ethyl (**6**)
butyl (**7**)

73

74

75

76

77 **Experimental Section**

78 **General**

79   All manipulations were carried out using standard Schlenk techniques under a nitrogen

80 atmosphere. Solvents were dried according to established methods[40] and purged with high

81 purity nitrogen gas prior to use. Diethyl ether (Et_2O) and tetrahydrofuran (THF) were dried

82 over sodium wire and benzophenone, absolute ethanol (EtOH) was dried over magnesium

83 turnings/iodine, and dichloromethane (DCM) was dried over phosphorous pentoxide. All other

84 reagents were purchased commercially and used as received. All NMR spectra were recorded

85 using a Bruker Avance III 400 MHz spectrometer at ambient temperature. The ^1H NMR data

86 are reported as chemical shift (δ, ppm) and referenced to the solvent peak $CDCl_3$. The proton

87 decoupled ^{13}C NMR data are presented as chemical shift (δ, ppm) and referenced to the solvent

88 peak $CDCl_3$ with the specific carbon indicated in parentheses. The ^{13}C DEPT 135 NMR data,

89 which distinguishes between CH, CH_2 and CH_3, are listed as chemical shift (δ, ppm) and

90 positive (pos) or negative (neg) with the corresponding carbons in parentheses. The IR spectra

91 were recorded on a Perkin Elmer Attenuated Total Reflectance (ATR) spectrophotometer and

92 elemental analyses were performed on a LECO CHNS elemental analyzer, while the melting

93 points were determined using a Stuart Scientific melting point apparatus.

94

95 **Synthesis of precursor 2,6-pyridine-dimethylene-ditosylate (PMT).** Reported protocols for

96 the preparation of the pyridine-based ligands involve expensive starting materials like

97 2,6-bis(chloromethyl)pyridine, therefore an alternate synthetic route was followed to reduce

98 the costs. A more suitable starting material, 2,6-pyridine-dimethylene-ditosylate (PMT), was

99 employed which involves the use of cheaper reagents to prepare, and the method followed was

100 adapted from Reger *et al.*[41] To a 500 ml round bottom flask (RBF), a solution containing 8.0 g

101 (0.20 mol) of NaOH and 2.78 g (0.020 mol) of 2,6-pyridinedimethanol was prepared in 150 ml

102 THF/water (1:1). The solution was then cooled to 0 °C to which a mixture of *p*-toluenesulfonyl

103 chloride in 75 ml of THF was added. After stirring at room temperature for four hours, the

104 mixture was poured into 200 ml of water and extracted with 75 ml of dichloromethane (DCM)

105 and this was repeated three times. The organic phase was washed with a saturated NaCl

106 solution and distilled water, and dried with Na_2SO_4. The solvent was removed under vacuum

107 yielding a crystalline white product (6.57g, 73%). ^1H NMR (400 MHz, $CDCl_3$): δ 2.4 (s, 6H),

108 5.1 (s, 4H), 7.3 (d, 6H), 7.7 (t, 1H), 7.8 (d, 4H).

109 **Synthesis of 2,6-bis(CH₃SCH₂)pyridine (L1).** To prepare this ligand a modified protocol

110 adapted from Canovese *et al.* was followed.[31] To a 50 ml two neck RBF fitted with a nitrogen

111 tap, a mass of 1.79 g of PMT was dissolved in ~40 ml of THF and this solution was cooled in

112 an ice bath. A mass of 0.62 g of sodium methanethiolate was added to the ice cooled solution

113 after which the mixture was stirred for 2 hours at room temperature. At the end of the reaction

114 the solvent was evacuated under reduced pressure and the resulting cream residue was

115 partitioned between DCM (200 ml) and water (100 ml). After washing several times with

116 water, the organic phase was dried with $MgSO_4$ and the solvent removed to yield the product

117 as impure pale yellow oil. The product was purified by elution with DCM through silica

118 packed column (0.53 g, 66%). ^{1}H NMR (400 MHz, $CDCl_3$): δ 2.0 (s, 6H), 3.8 (s, 4H), 7.2 (d,

119 2H), 7.6 (t, 1H). ^{13}C NMR (400 MHz, $CDCl_3$): δ 15.2 (*CH₃*-S), 40.0 (py-*CH₂*-S), 121.1 (*CH*-

120 py), 137.3 (*CH*-py), 158.2 (*C*-py). [13]C DEPT 135 (400 MHz, $CDCl_3$): δ 15.2 (CH₃-S) neg,

121 40.0 (CH₂-S) pos, 121.1 (CH-py) neg, 137.3 (CH-py) neg. IR ν_{max} (cm⁻¹): 3058 (w), 2966 (m),

122 2914 (m), 2856 (m), 1589 (s), 1572 (s), 1451 (s), 747 (s), 813 (m).

123

124 **Synthesis of 2,6-bis(CH₂CH₃SCH₂)pyridine (L2).** The procedure followed for the synthesis

125 of **L2** was adapted from Teixidor *et al.*[35] with a few modifications. Sodium metal (0.23 g, 10

126 mmol) and ethanethiol (0.5 ml, 10 mmol) were stirred together in ethanol (10 ml) for 20 min in

127 a 20 ml Schlenk tube. This solution was added to another ethanol solution (50 ml) of PMT

128 (2.24 g, 5 mmol) in a 100 ml two neck RBF fitted with a nitrogen tap, and the reaction mixture

129 was left to reflux overnight. The solvent was removed *in vacuo* and the residue was extracted

130 twice with diethyl ether (150 ml) and the remaining residue was discarded. The extract was

131 washed with aqueous Na_2CO_3 and twice with water (150 ml) and dried with $MgSO_4$. The

132 solvent was removed *in vacuo* to yield the impure product which was purified analogously to

133 **L1** to give a pale yellow oil (0.62 g, 54%). ^{1}H NMR (400 MHz, $CDCl_3$): δ 1.2 (t,6H), 2.5 (q,

134 4H), 3.8 (s,4H), 7.2 (d, 2H), 7.6 (t, 1H). ^{13}C NMR (400 MHz, $CDCl_3$): δ 14.5 (*CH₃*CH₂-S),

135 25.6 (CH₃*CH₂*-S), 37.8 (py-*CH₂*-S), 121.0 (*CH*-py), 137.2 (*CH*-py), 158.5 (*C*-py). [13]C DEPT

136 135 (400 MHz, $CDCl_3$): δ 14.5 (CH₃-S) neg, 25.6 (CH₂-S) pos, 37.8 (py-CH₂-S) pos, 121.0

137 (CH-py) neg, 137.2 (CH-py) neg. IR ν_{max} (cm⁻¹): 3056 (w), 2971 (m), 2926 (m), 2869 (m),

138 1590 (s), 1573 (s), 1451 (s), 747 (s), 788 (m).

139

140 **Synthesis of 2,6-bis(CH₂CH₂CH₂CH₃SCH₂)pyridine (L3).** A similar procedure to that for

141 **L2** was followed for **L3** with the following masses and volumes: sodium metal (0.14 g, 6.18

142 mmol), butanethiol (0.7 ml, 6.18 mmol), PMT (1.38 g, 3.09 mmol). No further purification was

143   required as the TLC showed only one spot; however the oil was dried under reduced pressure

144   for several hours to remove any solvent, thus yielding the product as a yellow oil (0.55 g,

145   63%). ^{1}H NMR (400 MHz, CDCl$_3$): δ 0.9 (t, 6H), 1.4 (m, 4H), 1.6 (m, 4H), 2.5 (t, 4H), 3.8 (s,

146   4H), 7.3 (d, 2H), 7.6 (t, 1H). ^{13}C NMR (400 MHz, CDCl$_3$): δ 13.7 ($CH_3CH_2CH_2CH_2$-S), 22.0

147   (CH$_3$$CH_2CH_2CH_2$-S), 31.3 (CH$_3CH_2$$CH_2CH_2$-S), 31.4 (CH$_3CH_2CH_2$$CH_2$-S), 38.1 (py-$CH_2$-S),

148   121.0 (CH-py), 137.2 (CH-py), 158.5 (C-py). ^{13}C DEPT 135 (400 MHz. CDCl$_3$): δ 13.7 (CH$_3$-

149   S) neg, 22.0 (CH$_2$-S) pos, 31.4 (CH$_2$-S) pos, 38.1 (CH$_2$-S) pos, 121.0 (CH-py) neg, 137.2 (CH-

150   py) neg. IR ν$_{max}$ (cm^{-1}): 3056 (w), 2956 (m), 2926 (m), 2871 (m), 1589 (s), 1573 (s), 1451 (s),

151   747 (s), 812 (m).

152

153   **Synthesis of 2,6-bis(C$_6$H$_5$SCH$_2$)pyridine (L4).** This method was adapted from Teixidor *et*

154   *al.*[37] Sodium metal (0.14 g, 6 mmol) was stirred with thiophenol (0.61 ml, 6 mmol) in ethanol

155   (10 ml) in a 20 ml Schlenk tube for 10 min. The solution was then added dropwise to an ice

156   cooled solution of PMT (1.52 g, 3 mmol) in THF (20 ml) and the resultant solution was stirred

157   for a further three hours at 0 °C. The solvent was then removed *in vacuo* and the resulting

158   residue was extracted with 70 ml diethyl ether and washed with 1 M NaOH solution (25 ml x

159   2) after which the organic layer was dried with MgSO$_4$. The solvent was removed *in vacuo* to

160   yield the product as pale yellow oil and no further purification was required (0.90 g, 82%). ^{1}H

161   NMR (400 MHz, CDCl$_3$): δ 4.2 (s, 4H), 7.1 (d, 4H), 7.2 (t, 4H), 7.3 (d, 4H), 7.5 (t, 1H). ^{13}C

162   NMR (400 MHz, CDCl$_3$): δ 40.3 (py-CH_2-S), 121.3 (CH-py), 126.2 (CH-ph), 128.9 (CH-ph),

163   129.6 (CH-ph), 135.7 (C-ph), 137.2 (CH-py), 157.3 (C-py). ^{13}C DEPT 135 NMR (400 MHz.

164   CDCl$_3$): δ 40.3 (py-CH$_2$-S) pos, 121.3 (CH-py) neg, 126.2 (CH-ph) neg, 128.9 (CH-ph) neg,

165   129.6 (CH-ph) neg, 137.2 (CH-py) neg. IR ν$_{max}$ (cm^{-1}): 3064 (w), 2962 (m), 2923 (m), 1590

166   (s), 1571 (s), 1450 (s), 1436 (s), 737 (s), 809 (m).

167

168   **Synthesis of 2,6-bis(C$_6$H$_{11}$SCH$_2$)pyridine (L5).** This method was adapted from Temple *et*

169   *al.*[42] In a 20 ml Schlenk tube, NaOH (0.32 g, 8.2 mmol) and cyclohexylmercaptan (1.0 ml, 8.2

170   mmol) were stirred together in ethanol (10 ml) for 30 min. This mixture was added dropwise to

171   a THF solution (20 ml) of PMT (1.79 g, 4 mmol) in a 100 ml two neck RBF fitted with a

172   nitrogen tap. After stirring at room temperature overnight, the solvent was removed *in vacuo*

173   and the residue was partitioned between DCM and deionized water (50 ml each). The organic

174   layer was collected, while the aqueous layer was washed with DCM (20 ml x 3), then the

175   organics were combined and dried with MgSO$_4$. After the solvent was removed *in vacuo* the

176   product was obtained as yellow oil and no further purification was required (1.21 g, 91%). ^{1}H

177   NMR (400 MHz, CDCl$_3$):δ 1.3 (m, 10H), 1.6 (m, 2H), 1.7 (m, 4H), 1.9 (m, 4H), 2.6 (m, 2H),

178   3.8 (s, 4H), 7.2 (d, 2H), 7.6 (t, 1H). ^{13}C NMR (400 MHz, CDCl$_3$): δ 25.9 (*CH$_2$*-cy), 26.1 (*CH$_2$*-

179   cy), 33.5 (*CH$_2$*-cy), 36.6 (py-*CH$_2$*-S), 43.4 (*CH*-cy), 121.0 (*CH*-py), 137.3 (*CH*-py), 158.8 (*C*-

180   py). ^{13}C DEPT 135 NMR (400 MHz. CDCl$_3$): δ 25.9 (CH$_2$-cy) pos, 26.1 (CH$_2$-cy) pos, 33.5

181   (CH$_2$-cy) pos, 36.6 (py-CH$_2$-S) pos, 43.4 (CH-cy) neg, 121.0 (CH-py) neg, 137.3 (CH-py) neg.

182   IR v$_{max}$ (cm^{-1}): 3064 (w), 2962 (m), 2923 (m), 1590 (s), 1571 (s), 1480 (s), 1449 (s), 737 (s),

183   809 (m).

184

185   **Synthesis of bis(CH$_2$CH$_3$SCH$_2$CH$_2$)amine (L6).** The method for the preparation of **L6** was

186   adapted from Konrad *et al*.[34] In a 250 ml Schlenk flask, a mass of 8.79 g (50 mmol) of bis(2-

187   chloroethyl)amine hydrochloride was dissolved in 100 ml of ethanol. The solution was added

188   to a 500 ml Schlenk flask which contained a mixture of NaOH (5.99 g, 150 mmol) and

189   ethanethiol (11.0 ml, 150 mmol) in ethanol (150 ml) at 0 °C. The resultant mixture was stirred

190   for two hours, filtered via cannula and the filtrate was dried *in vacuo*. Diethyl ether was added

191   to the residue and once again the mixture was filtered and the filtrate dried *in vacuo* to yield the

192   product as a pale yellow oil (6.66g, 69%). ^{1}H NMR (400 MHz, CDCl$_3$): δ 1.3 (t, 6H), 1.8 (s,

193   1H, N−H), 2.6 (q, 4H), 2.7 (t, 4H), 2.8 (q, 4H). ^{13}C NMR (400 MHz, CDCl$_3$): δ 14.9 (*CH$_3$*CH$_2$-

194   S), 25.9 (CH$_3$*CH$_2$*-S), 31.9 (*CH$_2$*CH$_2$-N), 48.3 (CH$_2$*CH$_2$*-N). ^{13}C DEPT 135 NMR (400 MHz.

195   CDCl$_3$): δ 14.9 (CH$_3$-S) neg, 25.9 (CH$_2$-S) pos, 31.9 (CH$_2$-N) pos, 48.3 (CH$_2$-N) pos. IR v$_{max}$

196   (cm^{-1}): 3288 (w), 2962 (s), 2921 (s), 2864 (s), 2823 (s), 1451 (s), 739 (m).

197

198   **Synthesis of bis(CH$_2$CH$_2$CH$_2$CH$_3$SCH$_2$CH$_2$)amine (L7).** **L7** was synthesised analogously to

199   **L8** with the following masses and volumes: bis(2-chloroethyl)amine hydrochloride (8.81 g, 50

200   mmol), NaOH (6.13 g, 150 mmol) and butanethiol (16.0 ml, 150 mmol). The product was

201   obtained as yellow oil (10.71 g, 86%). ^{1}H NMR (400 MHz, CDCl$_3$): δ 0.9 (t, 6H), 1.3 (m, 4H),

202   1.5 (m, 4H), 1.8 (s, 1H, N−H), 2.5 (t, 4H), 2.6 (t, 4H), 2.8 (t, 4H). ^{13}C NMR (400 MHz,

203   CDCl$_3$): δ 13.7 (*CH$_3$*CH$_2$CH$_2$CH$_2$-S), 22.0 (CH$_3$*CH$_2$*CH$_2$CH$_2$-S), 31.7 (CH$_3$CH$_2$*CH$_2$*CH$_2$-S),

204   31.8 (CH$_3$CH$_2$CH$_2$*CH$_2$*-S), 32.4 (*CH$_2$*CH$_2$-N), 48.4 (CH$_2$*CH$_2$*-N). ^{13}C DEPT 135 NMR (400

205   MHz. CDCl$_3$): δ 13.7 (CH$_3$-S) neg, 22.0 (CH$_2$-S) pos, 31.7 (CH$_2$-S) pos, 31.8 (CH$_2$-S) pos,

206   32.4 (CH$_2$-N) pos, 48.4 (CH$_2$-N) pos. IR v$_{max}$ (cm^{-1}): 3294 (w), 2955 (vs), 2925 (vs), 2872 (vs),

207   1458 (s), 741 (m).

208

209   **Synthesis of Co[2,6-bis(CH$_3$SCH$_2$)pyridine]Cl$_2$ (1).** A mixture of **L1** (0.4917 g, 2.5 mmol) in

210   ethanol (5 ml) was added dropwise to a solution of CoCl$_2$.6H$_2$O (0.5717 g, 2.4 mmol) in

ethanol (10 ml) in an almost 1:1 mole ratio with the ligand in slight excess. After an overnight reflux, the resulting indigo solution was concentrated by reducing the volume of the solvent to ~5 ml. At this point the product precipitated out, was separated via cannula filtration and washed with a small amount of ethanol. Drying *in vacuo* for several hours afforded the product as a blue microcrystalline solid (0.28 g, 36%). Crystals suitable for X-ray diffraction were grown from a concentrated acetonitrile solution layered with Et_2O. Elemental analysis for $C_9H_{13}Cl_2CoNS_2$: calcd C, 32.8; H, 4.0; N, 4.3; found C, 32.4; H, 4.4; N, 4.0. Melting point: 176-177 (dimer), 196-197°C.

Synthesis of Co[2,6-bis(CH$_2$CH$_3$SCH$_2$)pyridine]Cl$_2$ (2). Complex **2** was prepared analogously to **1** using 0.1235 g (0.52 mmol) of $CoCl_2.6H_2O$ and 0.1193 g (0.53 mmol) **L2**. A brilliant blue crystalline solid was obtained (0.086 g, 47%). Crystals suitable for X-ray diffraction were deposited from a concentrated ethanol solution. Elemental analysis for $C_{11}H_{17}Cl_2CoNS_2$: calcd C, 37.0; H, 4.8; N, 3.9; found C, 37.3; H, 5.2; N, 3.9. Melting point: 164-165°C.

Synthesis of Co[2,6-bis(CH$_2$CH$_2$CH$_2$CH$_3$SCH$_2$)pyridine]Cl$_2$ (3). Complex **3** was prepared analogously to **1** using 0.0843 g (0.35 mmol) of $CoCl_2.6H_2O$ and 0.1021 g (0.36 mmol) of **L3**. An indigo blue crystalline solid was obtained (0.069 g, 48%). Crystals suitable for X-ray diffraction were grown from a concentrated ethanol solution. Elemental analysis for $C_{13}H_{21}Cl_2CoNS_2$: calcd C, 44.5; H, 6.8; N, 3.1; found C, 45.0; H, 6.6; N, 3.4. Melting point: 107-108°C.

Synthesis of Co[2,6-bis(C$_6$H$_5$SCH$_2$)pyridine]Cl$_2$ (4). Complex **4** was prepared analogously to **1** using 0.1190 g (0.50 mmol) of $CoCl_2.6H_2O$ and 0.1635 g (0.51 mmol) of **L4**. An aqua blue powder was obtained (0.17 g, 77%). Crystals suitable for X-ray diffraction were grown by vapor diffusion of Et_2O into a concentrated DCM solution. Elemental analysis for $C_{19}H_{17}Cl_2CoNS_2$: calcd C, 50.3; H, 3.8; N, 3.1; found C, 50.1; H, 4.3; N, 3.0. Melting point: 211-213°C.

Synthesis of Co[2,6-bis(C$_6$H$_{11}$SCH$_2$)pyridine]Cl$_2$ (5). Complex **5** was prepared analogously to **1** using 0.1188 g (0.50 mmol) of $CoCl_2.6H_2O$ and 0.1717 g (0.51 mmol) of **L5**. A fine purple powder was obtained (0.10 g, 43%). Elemental analysis for $C_{19}H_{29}Cl_2CoNS_2$: calcd C, 49.0; H, 6.3; N, 3.0; found C, 48.6; H, 6.8; N, 2.8. Melting point: 142-143 °C.

245

246   **Synthesis of Co[bis(CH$_2$CH$_3$SCH$_2$CH$_2$)amine]Cl$_2$ (6).** A mixture of **L6** (0.2448 g, 1.26

247   mmol) in ethanol (5 ml) was added dropwise to a solution of CoCl$_2$.6H$_2$O (0.2615 g, 1.09

248   mmol) in ethanol (10 ml) in an almost 1:1 mole ratio, with the ligand in slight excess, and a

249   color change from dark blue to indigo-purple was observed. The reaction mixture was allowed

250   to stir for two hours at room temperature after which the solution was concentrated to ~5 ml

251   and the product precipitated out as a lavender colored solid which was separated via cannula

252   filtration (0.23 g, 66%). Elemental analysis for C$_8$H$_{19}$Cl$_2$CoNS$_2$: calcd C, 29.7; H, 5.9; N, 4.3;

253   found C, 29.6; H, 6.3; N, 4.2. Melting point: 171-172°C.

254

255   **Synthesis of Co[bis(CH$_2$CH$_2$CH$_2$CH$_3$SCH$_2$CH$_2$)amine]Cl$_2$ (7).** Complex **7** was prepared

256   similarly to **6** using 0.3061 g (1.29 mmol) of CoCl$_2$.6H$_2$O and 0.3606 g (1.45 mmol) of **L7**. A

257   lavender powder was obtained (0.31g, 64%). Elemental analysis for C$_{12}$H$_{27}$Cl$_2$CoNS$_2$: calcd C,

258   38.0; H, 7.2; N, 3.7; found C, 37.9; H, 7.6; N, 3.7. Melting point: 144-145°C.

259

260   **X-ray Structure determinations**

261   Single crystals were selected and glued onto the tip of a glass fiber, mounted in a stream of

262   cold nitrogen at 173 K and centered in the X-ray beam by using a video camera. Intensity data

263   were collected on a Bruker APEX II CCD area detector diffractometer with graphite

264   monochromated Mo K_α radiation (50 kV, 30 mA) using the APEX 2 data collection software.

265   The collection method involved ω-scans of width 0.5° and 512x512 bit data frames. Data

266   reduction was carried out using the program SAINT+ while face indexed and multi-scan

267   absorption corrections were made using SADABS. The structures were solved by direct

268   methods using SHELXS.[43] Non-hydrogen atoms were first refined isotropically followed by

269   anisotropic refinement by full matrix least-squares calculations based on F^2 using SHELXS.

270   Hydrogen atoms were first located in the difference map then positioned geometrically and

271   allowed to ride on their respective parent atoms. Diagrams were generated using SHELXTL,

272   PLATON[44] and ORTEP-3[45]. In preliminary refinements for complex **3** the butyl groups in the

273   structure were found to be disordered and were as a consequence refined over two positions

274   with isotropic thermal parameters. Carbon atoms in the butyl groups were refined isotropically

275   with a common U_{iso} parameter. Crystallographic data and additional information regarding the

276   crystal structure determination are available as supplementary material. Furthermore, CCDC

277   984366-984369 respectively for compounds **1-4** obtainable from the Cambridge

278   Crystallographic Data Centre contain supplementary crystallographic data for this contribution.

279

280   **Oxidation of *n*-octane**

281   The paraffin oxidation studies were carried out using *n*-octane as substrate with pentanoic acid

282   as internal standard. The catalytic reactions were performed under a nitrogen atmosphere in a

283   50 ml two-neck pear shaped flask equipped with a condenser. The reaction mixture consisted

284   of 5 ml degassed acetonitrile (solvent), TBHP as oxidant, *n*-octane and the respective catalyst

285   (3 mg). The reaction mixture was stirred in an oil bath at the optimum temperature (80 °C) and

286   after the time period (24 and 48 hours for the amine and pyridine-based catalysts respectively),

287   an aliquot of the sample was removed with a Pasteur pipette and filtered through a cotton wool

288   plug, after which 0.5 μL of the aliquot was injected into a GC for analysis and quantification.

289   Masses and volumes of components of the reaction mixture were dependent on the specific

290   catalyst; however catalyst loading was kept constant at 1 mol%, i.e. a catalyst to substrate mole

291   ratio of 1:100. Furthermore, *n*-octane to oxidant ratio was varied between 1:3, 1:6, 1:9, 1:12,

292   1:20, 1:30 and 1:40 from which the optimum ratio of 1:20 was established. At higher oxidant

293   concentrations, substrate reactivity decreased drastically indicating that the catalyst was

294   possibly deactivated by the excess oxidant in the reaction vessel. All reactions (including

295   blanks) were carried out in duplicates. The average conversion was expressed as a percentage

296   of total moles of products/initial moles of substrate, while selectivity was expressed as a

297   percentage of moles of each product/sum total moles of all products.

298   **Results and Discussion**

299   **Syntheses and characterization of new cobalt complexes**

300   In this study, the synthesis and application of seven new Co complexes containing SNS ligands

301   are reported in which two sets of ligands were synthesized based on variation in architecture of

302   the backbone N-donor atom, these are: (i) a constrained six-membered pyridine ring and (ii) a

303   linear straight chained amine. Synthesis of all ligands was adapted from literature, however

304   novel methodologies were developed for preparation of the SNS-Co(II) complexes

305   summarized in Scheme 1. Successful formation of products was monitored and confirmed by a

306   variety of techniques, discussed later. However, it is noted that due to the paramagnetic high

307 spin nature of the cobalt(II) complexes, their unresolved NMR data are not reported in this

308 study.

309 Refluxing the metal salt (CoCl$_2$.6H$_2$O) with isolated SNS ligands

310 {2,6-bis(RSCH$_2$)pyridine [R = methyl, **L1**; ethyl, **L2**; butyl, **L3**; phenyl, **L4** and cyclohexyl,

311 **L5]** and bis(RSCH$_2$CH$_2$)amine [R= ethyl, **L6** and butyl, **L7**]} afforded corresponding pyridyl-

312 centered SNS complexes Co[2,6-bis(RSCH$_2$)pyridine]Cl$_2$ (R = methyl, **1**; ethyl, **2**; butyl, **3**;

313 phenyl, **4** and cyclohexyl, **5**) and amine-based SNS complexes Co[bis(RSCH$_2$CH$_2$)amine]Cl$_2$

314 (R = ethyl, **6** and butyl, **7**). Initial indicators of complex formation were the absence of

315 resolvable NMR data combined with sharp melting points and distinct color changes during the

316 reaction. For the pyridyl complexes (**1**-**5**), accurate elemental analyses were combined with

317 data from X-ray diffraction (with the exception of **5**) for confirmation of molecular

318 composition, structure and geometry.

319 The amine-based complexes (**6**-**7**) were very air sensitive, comparatively less stable than the

320 corresponding pyridyl complexes (**2**-**3**) and decomposed on exposure to the atmosphere.

321 Hence, all attempts at growing crystals suitable for X-ray crystallography failed. However, data

322 from other techniques including IR, elemental analysis and melting point, conclusively

323 confirmed isolation of the intended complexes in high purity. Table 1 presents a summary of

324 the most important bands in the IR spectra which correspond to the N−H stretching vibration

325 (3500-3300 cm^{-1}), the C−H alkyl stretch and bend as well as C−H rocking vibrations.

326 However, IR spectroscopy was unsuitable for detecting the C−S stretch for all three ligands

327 due to overlap by strong and broad C−H rocking vibrations, but it is worth noting that the

328 signals did intensify upon ligand coordination to the Co center. Relevant shifts in vibration

329 frequencies, such as weakening of the N–H stretching frequency of **7** from 3294 to 3219 cm^{-1}

330 are interpreted as indicators of successful complexation of the SNS ligands to the metal center.

331

332 **Crystal structures of 1-4**

333 With the exception of the methyl substituted complex **1**, which was isolated as a chloro-

334 bridged bimetallic specie containing octahedrally bonded cobalt centers (Fig. 1), the longer

335 chain (S-bonded R substituents) analogues all crystallized with a trigonal bipyramidal

336 geometry around each cobalt(II) center (Figs. 2, 4 and 5) with selected bond lengths and bond

337 angles listed in Table 2. Consequently, **2**, **3** and **4** all crystallized in the monoclinic crystal

338 system, while **1** crystallized in the lower symmetry triclinic P-1 space group. The molecular

339 structure of **1**, as presented in Fig. 1, shows tridentate SNS ligands each chelated in a

340 meridional fashion to cobalt centers via two sulfur atoms and a nitrogen atom from the pyridine

341 ring. Relatively weak metal-metal interactions were observed between the two octahedral
342 centers of **1** separated through space by a Co---Co distance of 3.684 Å, which in perspective is
343 weaker than similar interactions in reported square-planar SNS metal complexes bearing *t*-
344 butyl groups on the S-donor atoms, having dimeric centers (respectively, 3.223 and 3.255 Å for
345 Ir---Ir and Rh---Rh).[36]

346 **Table 1:** Selected IR data for ligands and corresponding complexes **6** and **7**.

Ligand/ Complex	IR v_{max}/cm^{-1}			
	N−H stretch^a	C−H (alkyl)^b	C-H bend (alkyl)^b	C−S^a
L6	3228	2864	1458	N/A
6	3228	2870	1465	694
L7	3294	2872	1458	N/A
7	3219	2867	1464	744

347 ^{a} weak (for the coordinated S donor), ^{b} medium, ^{c} strong.

348
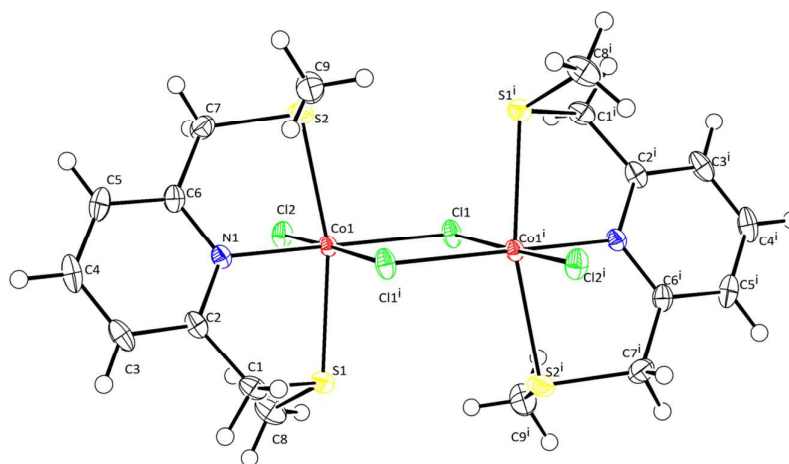
349

350 **Figure 1:** Molecular structure and atomic numbering scheme of **1** with thermal ellipsoids at the
351 50% probability level.

352

353 **Table 2:** Selected bond lengths (Å) and bond angles (°) for **1-4**

	1	2	3	4
N(1)–Co(1)	2.1131(17)	2.048(7)	2.133(3)	2.057(5)
S(1)–Co(1)	2.4980(5)	2.521(2)	2.4496(15)	2.5460(17)
S(2)–Co(1)	2.4889(6)	2.518(3)	2.4604(14)	2.5208(17)
S(2)–Co(1)–S(1)	162.85(2)	161.90(8)	152.55(7)	161.84(6)

12

| N(1)–Co(1)–S(1) | 81.84(5) | 82.3(2) | 152.55(7) | 81.94(15) |
| N(1)–Co(1)–S(2) | 81.33(5) | 81.5(2) | 80.80(10) | 81.13(14) |

354

355

356 Complex **2** crystallizes in the monoclinic *Cc* space group with four twins (independent

357 molecules A & B, Fig. 2) in the asymmetric unit cell. The Co(II) ion in each molecule exists as

358 a five coordinate center stabilized by the neutral SNS ligand and two terminal chloride ions.

359 Due to the increased size of the S-atom substituent (R group), the geometries of latter members

360 of this series of complexes differ significantly in solid state structural conformations when

361 compared to **1**. This is due to the non-constrained free rotation around C–C single bonds that

362 result in increased steric bulk and less compact geometries. For instance, the bulkier and

363 electronically richer ethyl R group in **2** may be partly responsible for its propensity to exist as a

364 five coordinate monomer, while **1** easily dimerizes in an octahedral fashion. A comparison of

365 selected bond lengths and angles shows that the N(1)–Co(1) bond of **2** is shorter than that of **1**

366 [2.048(7) Å vs. 2.1131(17) Å], while the S(1)–Co(1) and S(2)–Co(1) bond lengths are longer,

367 indicative of a stronger C–N bond and comparatively weaker C–S bonds in **2**. This observation

368 may be ascribed to increased back-donation and overlap of d-orbitals of the Co(II) center and

369 the pi-anti bonding orbitals of the pyridyl N-donor as a result of the ethyl group in **2**.
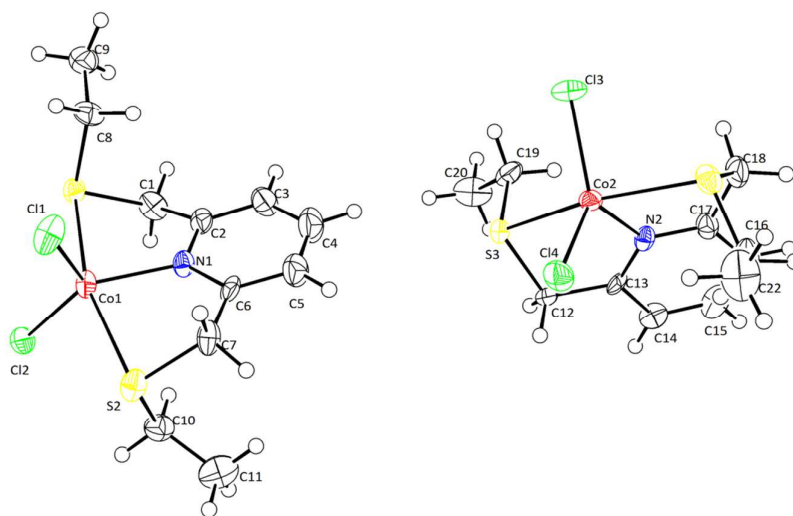
370

371

372

373

374

375

376

377

378

379

380

381

382 **Figure 2:** Molecular structure and atomic numbering scheme of **2** showing two

383 crystallographically independent molecules (A & B) in the asymmetric unit cell. Thermal

384 ellipsoids are drawn at the 50% probability level.

385

386   A distorted trigonal bipyramidal geometry is observed for **2** due to a slightly narrower 'bite
387   angle' defined as the S(2)–Co(1)–S(1) angle. The geometry around the metal center is defined
388   by three equatorial positions occupied by the two chlorides and the N-donor atom, while the
389   two axial positions are occupied by the relatively *trans* S-donor atoms. A related Zn(SNS)
390   complex reported by Teixidor and co-workers[35] revealed a conformation similar to **2**, but, due
391   to the presence of bulkier bromide ions, exhibited an acute S(1)–Zn–S(2) bite angle of 157.0°,
392   compared to 161.90° for **2**.
393   Observation of the crystal packing between molecules of **2** revealed an ordered arrangement of
394   crystal units containing A and B molecules in alternating planes (Fig. 3), which resulted in a
395   higher melting point of 164-165° compared to 107-108° for **3** . Primarily, the more ordered
396   crystal in the solid state required a greater input of energy to disrupt intermolecular cohesion in
397   the complex.[46]
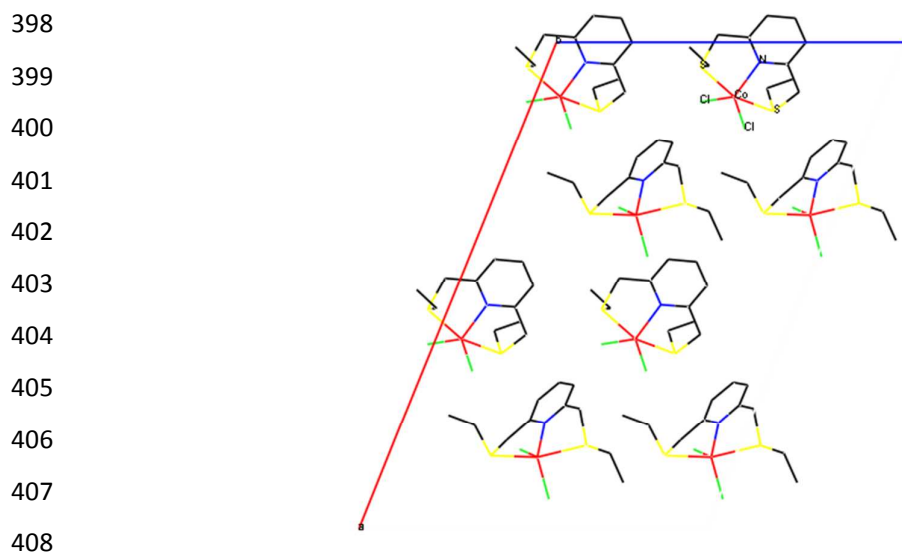
409   **Figure 3:** Wireframe representation of the crystal packing of **2** with hydrogen atoms omitted
410   for clarity**.**

411

412   Geometrically, complex **3** (Fig. 4) is very similar to **2** with distorted trigonal bipyramidal
413   geometry in which the pyridyl moiety and the two chloride groups occupy equatorial positions,
414   while the two S-donor atoms occupy axial positions. The N(1)–Co(1), S(1)–Co(1) and S(2)–
415   Co(1) bond lengths for **3** are very similar to **1** (Table 2), but a noticeably more acute bite angle
416   of 152.55(7)° is observed in comparison to either **1** or **2**. The pyridyl ring is twisted such that
417   C(2) and C(6) reside on the S-N-S-Co plane, whereas C(3), C(4) and C(5) atoms deviate from
418   the [N(1), C(2), C(3), C(4), C(5)] plane by 0.383, 0.485 and 0.313 Å respectively, leading to a
419   dihedral angle of 11.81°.
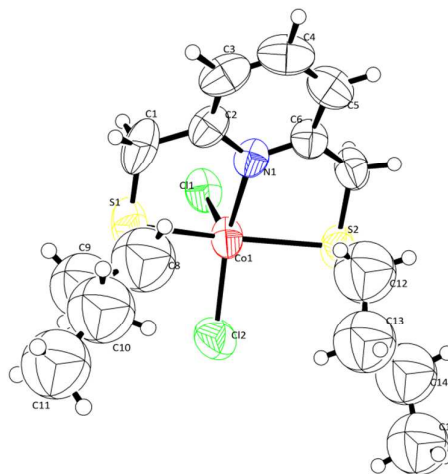
Figure 4: Molecular structure and atomic numbering scheme of **3** showing one conformation of the disordered butyl group with thermal ellipsoids at the 50% probability level.

Unlike in complexes **1** and **2**, the substituent 'arms' C(1) and C(7) are positioned on the same side of the S-N-S-Co plane, deviating by just 0.155 and 0.287 Å respectively. The steric bulk and disorder brought about by the free rotation of the butyl groups accounted for the relatively low melting point (107-108 °C) for **3** compared to the other complexes reported herein.[46]
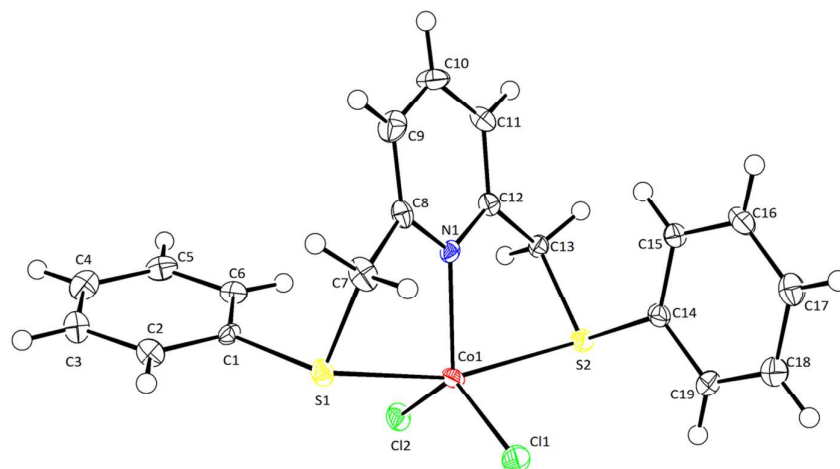
Figure 5: Molecular structure and atomic numbering scheme of **4** with thermal ellipsoids at the 50% probability level.

454   Complex **4**, represented in Fig. 5, crystalizes in the P21/c space group with the phenyl

455   substituents positioned on opposite sides of the S-N-S-Co plane, which correlates to a related

456   Cr complex reported by Temple et al.[42] In comparison to **3**, the methylene linkers C(7) and

457   C(13) are situated on either side of S-N-S-Co plane deviating from the plane by +0.950 and -

458   0.825 Å respectively.

459

Application of complexes 1-7 in the oxidation of *n*-octane

461   As noted earlier, the main goal of this study was to prepare catalysts for the selective activation

462   of paraffins represented by *n*-octane. To test the effectiveness of complexes **1-7**, *tert*-butyl

463   hydroperoxide (TBHP) was used as a source of oxygen for the *n*-octane. The choice of the

464   oxidant was based on the knowledge that it is a more effective and milder source of reactive

465   oxygen as compared to the more common hydrogen peroxide (H_2O_2).[47,48] Exploratory work

466   with the current set of catalysts has also showed that TBHP is the more active and stable source

467   of oxygen, hence all data presented here are based on its use as the oxidant.

468   A series of exploratory experiments were conducted in order to establish optimum reaction

469   conditions for optimal substrate conversion and product selectivity. The optimum octane to

470   oxidant ratio was found to be 1:20 while 24 and 48 hours were the most favorable reaction

471   times for the amine- and pyridine-based complexes respectively. Results showed that beyond

472   these time frames no significant change in substrate conversion was obtained. Furthermore, too

473   low conversions were observed at shorter reaction times. Blank reactions with only the oxidant

474   TBHP in the absence of any catalyst gave a total *n*-octane conversion of 1% and as expected,

475   no conversion was observed for blank runs that contained the catalyst in the absence of any

476   oxidant. A blank run with metal precursor ($CoCl_2.6H_2O$) as the catalyst was also performed

477   and the results revealed 5 and 7% *n*-octane conversions after 24 and 48 hours respectively.

478   Furthermore, only 2-,3- and 4-octanone were formed and no 1-octanol or other products of

479   primary carbon activation were detected, indicating poor selectivity to primary products for the

480   blank runs.

481

482   The oxidation of *n*-octane with catalysts **1-7** at the optimum conditions produced a mixture of

483   isomeric octanones and octanols that were oxygenated at carbon positions 1, 2, 3 and 4

484   (Scheme 2), as well as other terminal products, mainly octanal and octanoic acid. Furthermore,

485   no cracking of the substrate was observed and only C8 products were obtained. Table 3

486   presents data on total octane conversion and the regioselectivity parameter (C1:C2:C3:C4).

487   The regioselectivity parameter compares relative reactivity of hydrogen atoms at carbon

488   positions 1, 2, 3 and 4 along the *n*-octane backbone leading to various oxygenates (Scheme 2).

489   Results of the catalytic study suggest that amongst the pyridine-based catalysts, **1** was the most

490   active, with the highest (12%) total conversion of the substrate *n*-octane. Such an outcome was

491   not unexpected considering that **1** has the least sterically hindered active site due to the

492   relatively small methylene groups bonded to the ligand S-donor atoms. This, in theory, should

493   render greater access to the metal center for the substrate and lead to the enhanced catalytic

494   activity observed for **1**. In general terms, there is an inverse relationship between reactivity of

495   the metal complexes and size of the R group on the S-donor atoms, which implies that catalytic

496   activity is dominated by steric factors.

497

498   Scheme 2: **Product distribution in the oxidation of *n*-octane**
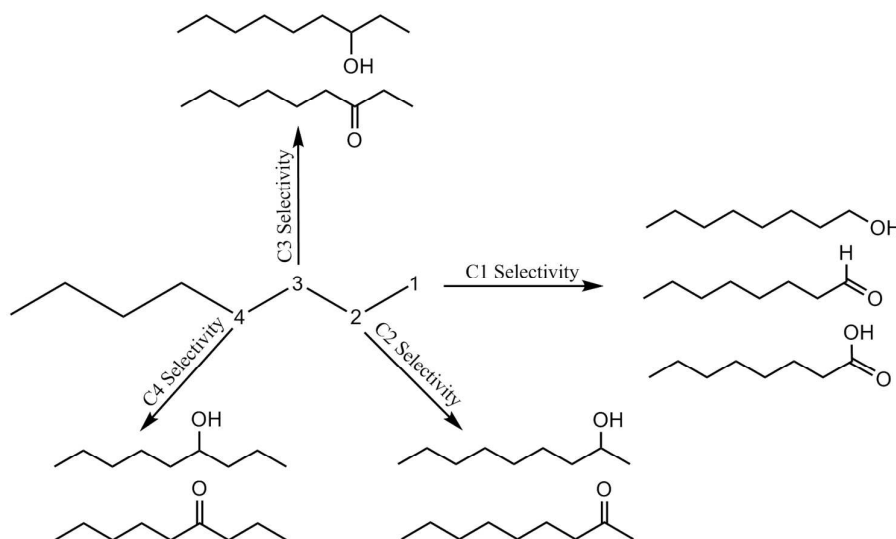
499

500

501   However, in the instances where the side groups are straight chain alkyl substituents, electronic

502   and steric contributions to reactivity are difficult to separate because the longer chain members

503   show enhanced electronic contributions to the chelating S-donors, but are also the more

504   sterically hindered. The question that arose in these instances is whether sterics or electronics

505   dominate the activity of the catalysts. Complexes **4** and **5** contain phenyl and cyclohexyl side

506   groups respectively and the difference in reactivity between these two catalysts led to the belief

507   that steric access to the metal center is the prime determinant of catalytic activity. The planar

508   phenyl side group in **4** is less sterically demanding than the electronically richer but sterically

509 bulkier cyclohexyl in **5**. The result is consistent and showed better total conversion and

510 selectivity for **4**.

511 In addition to R-group steric variation as a determinant of catalytic activity in complexes **1**-**5**,

512 the amine N-donor containing complexes (**6** and **7**) displayed significantly higher catalytic

513 activities with conversions of 23 and 17% respectively which is likely due to additional

514 flexibility of the amine backbone. This observation has implications for the design of catalysts

515 stabilized by carbon chain chelated donor atoms.

516 **Table 3:** Total conversion and regioselectivity parameter C1:C2:C3:C4 in the oxidation of

517 *n*-octane using TBHP as oxidant.

Catalyst	Total conversion/%	Octanone selectivity/%	Octanol C1:C2:C3:C4	Octanone C2:C3:C4	Total[a] C1:C2:C3:C4
1	12	83	1:3.5:3.1:0	1.3:1:1	1:5.8:4.6:3.7
2	11	79	1:1.7:0:1.9	1.5:1.1:1	1:3.9:2.5:2.8
3	9	83	2:3.6:1:3.6	1.4:1:1	1:5.6:3.9:4.2
4	9	82	1:1.5:0:2.5	1.4:1:1	1:3.8:2.6:3.2
5	7	77	1:2.5:0:5	1.4:1:1	1:4.7:3.2:4.1
6	23	83	1:1.9:2.1:1.4	1.4:1.1:1	1:4.1:3.3:3.0
7	17	90	1:1:0:3.3	1.4:1.1:1	1:8.3:6.4:6.4

518 [a] Total regioselectivity parameter takes into account all products (octanones, octanols, octanal and octanoic acid).

519 Reactions were carried out at 80 °C with a catalyst loading of 1 mol%, octane to oxidant ratio of 1:20, pentanoic

520 acid as the internal standard and reaction times of 24 and 48 hours for the amine- and pyridine-based catalysts

521 respectively.

522

523 The degree of flexibility of the carbon chain linker between the chelated donor atoms is

524 important for the set of SNS ligands reported herein. A flexible two carbon spacer between a

525 simple amine N-donor and the S-donor atoms yielded more effective catalysts than a rigid

526 pyridine N-donor linked to the S-donors via a methylene spacer. Direct comparison of the two

527 structurally related amine backbone complexes **6** (SNS-etamine) and **7** (SNS-butamine) further

528 confirmed the importance of side chain steric influence as a key determinant of catalytic

529 activity. Hence in summary, complex **6** functionalized by a relatively smaller ethyl R group

530 showed the best potential for *n*-octane oxidation amongst the whole range of seven catalysts

531 studied.

532 Consistent with reported observations, total regioselectivity for each catalyst (Table 3) showed

533 that internal hydrogens at carbon position C2 (Scheme 2) were the most reactive, while

534 terminal hydrogens at position C1 were the least reactive.[1,47] Hence, total selectivity up to 90%

535 was recorded for octanone isomers via activation of internal carbon positions (mainly C2 but

536   also including C3 and C4) as the dominant products of the oxidation reaction which is an

537   improvement over the selectivity of ca. 80% previously reported by Pombeiro *et al.*[47]

538   Specifically on octanols, it was observed that the highest selectivity to 1- and 2-octanols was

539   displayed by **3**, 3-octanol by **1** and 4-octanol by **5**, implying that the more rigid pyridine N-

540   donor based complexes are more selective against over-oxidation of octanols to octanones as

541   compared to complexes **6** and **7**. However, it is evident that overall **7** displayed the highest

542   selectivity at positions C2, C3 and C4 which accounted for the higher overall octanone

543   production at these positions. The trends of these parameters are comparable to those reported

544   in the literature[47, 49] for catalytic systems that utilized TBHP as the oxidant. Furthermore, these

545   results imply that a radical initiated mechanism is followed as proposed by Pombeiro and co-

546   workers.[47]

547   Thus far it is safe to summarize that in these catalytic systems, over-oxidation of internal

548   carbons has led to the production of ketones as the main dominant products. In an effort to

549   further understand the rate of this oxidation of alcohols to ketones, an experiment was set up

550   under similar conditions as used for the octane oxidation. Complex **6** was used as a

551   representative catalyst, into which a fresh solution of 2-octanol was oxidized with TBHP over a

552   5 hr period. The result revealed a time dependent production of over 86% 2-octanone within

553   the 5 hr period. This observation suggests that the overoxidation of octanols (including 1-

554   octanol to octanal) proceeded quite early and relatively quickly in the current systems such that

555   any alcohol that was formed almost immediately got further oxidized. To put the results of this

556   catalytic study into context, closely related literature are summarized below:

557   • Kirillova *et al*. have described the use of a tetracopper(II) complex for the oxidation of

558   alkanes under mild conditions using TBHP as the oxidant.[49] The results obtained for

559   the oxidation of *n*-octane in particular showed that the reaction did not involve free

560   hydroxyl radicals due to the high regioselectivity profile (1:65:32:30) after 30 min

561   reaction time. Following an increase in the reaction time to 180 min, the parameter

562   dropped to 1:10:6:6. In addition, over-oxidation of alcohols to the corresponding

563   ketones was observed.

564   • Lau and co-workers have reported on the oxidation of alkanes by an $[Os^{VI}(N)Cl_4]^-$

565   /Lewis acid system using various peroxides including TBHP.[50] Yields of up to 93%

566   based on [TBHP] consumption were obtained with *cyclohexane* as the substrate. A

567   yield of up to 69% alcohol production was achieved and further oxidation of the

568   alcohol to cyclohexanone was also observed. Studies using open-chain alkanes (*n*-
569   hexane and *n*-heptane) as substrates were also carried out but no oxidation of the
570   primary C–H bond was achieved although total yields of up to 83% were obtained.

571   • Shul'pin *et al.* have demonstrated the oxidation of a variety of substrates using a
572   manganese(IV) complex salt.[48] In particular, the results obtained for the oxidation of *n*-
573   octane with TBHP showed the production of a mixture of isomeric alcohols and
574   ketones, with negligible activation of the primary C–H bond.

575   • Pombeiro, Shul'pin and co-workers have reported a tetracopper(II) triethanolaminate
576   complex for the oxidation of alkanes using H_2O_2 and acid co-catalysts.[51] For *n*-octane,
577   regioselectivity parameters of 1:4.3:3.7:3.4 and 1:5.1:5.2:4.3 were reported.

578   • Pombeiro *et al.* have also described the oxidation of alkanes using a homogeneous and
579   immobilized Mn(salen) complex.[47] The results obtained for the oxidation of *n*-octane
580   with TBHP are as follows: no activation of the primary C–H bond was observed,
581   isomeric alcohols and ketones were formed which were oxygenated at positions 2, 3
582   and 4 of the hydrocarbon chain and yields of ca. 1% were reported with TONs of up to
583   110. Furthermore, low regioselectivity profiles [C(2):C(3):C(4)] of 1:1:1.3 and
584   1.7:1:1.1 for the homogeneous and immobilized catalysts respectively, were obtained.

585   • Finally, a report from Pombeiro, Shul'pin and co-workers have described the oxidation
586   of alkanes using a H_2O_2-$NaVO_3$-H_2SO_4 catalyst system.[52] Regioselectivity parameters
587   of 1:10.1:10.7:8.4 and 1:7:6:5 were obtained for this system in MeCN and H_2O
588   respectively.

589

590 Conclusion

591 The preparation of a series of cobalt complexes containing pincer-type SNS ligands with two
592 different backbones: a constrained six-membered pyridine ring and a linear straight chained
593 amine have been achieved. The crystal structures of complexes **1**-**4** confirmed that the SNS
594 ligands were terdentate and coordinated to the metal centre via the N- and S-donor atoms.
595 All the Co complexes (**1**-**7**) were tested for the oxidative functionalization of *n*-octane with
596 TBHP as the oxidant. Only linear C8 oxygenated products were obtained. Complex **1** was the
597 most active catalyst in the pyridine-based series with a total conversion of 12%, while **6** was

598 the most active amongst the two amine-based catalysts with a recorded total conversion of

599 23%. Overall, the amine-based complexes proved to be the most efficient catalysts in this

600 study, as significantly higher conversions were exhibited compared to the pyridine-based

601 catalysts. But, the more rigid pyridine-based complexes showed better alcohol selectivity.

602 According to the selectivity profile for each catalyst, octanones were more abundant, with

603 2-octanone being the dominant product formed, which is in line with the regioselectivity

604 parameter that revealed C2 as the prominent position of attack on the hydrocarbon chain for all

605 the catalysts studied.

606

Acknowledgements

611

References

613 1.   J. A. Labinger and J. E. Bercaw, *Nature*, 2002, **417**, 507-514.
614 2.   B. C. Bailey, H. Fan, J. C. Huffman, M.-H. Baik and D. J. Mindiola, *J. Am. Chem. Soc.*,
615   2007, **129**, 8781-8793.
616 3.   J. Brazdil, *Topics in Catalysis*, 2006, **38**, 289-294.
617 4.   A. E. Shilov and G. B. Shul'pin, *Chem. Rev.*, 1997, **97**, 2879-2932.
618 5.   R. H. Crabtree, *J. Chem. Soc., Dalton Trans.*, 2001, 2437-2450.
619 6.   R. H. Crabtree, *J. Organomet. Chem.*, 2004, **689**, 4083-4091.
620 7.   G. W. Parshall, *Acc. Chem. Res.*, 1975, **8**, 113-117.
621 8.   Y. N. Kozlov, G. V. Nizova and G. B. Shul'pin, *J. Phys. Org. Chem.*, 2008, **21**, 119-
622   126.
623 9.   J. A. Labinger, *Fuel Process. Technol.*, 1995, **42**, 325-338.
624 10.   T. A. van den Berg, J. W. de Boer, W. R. Browne, G. Roelfes and B. L. Feringa, *Chem.
625   Commun.*, 2004, 2550-2551.
626 11.   G. B. Shul'pin, *C.R. Chim.*, 2003, **6**, 163-178.
627 12.   A. Vigalok, O. Uzan, L. J. W. Shimon, Y. Ben-David, J. M. L. Martin and D. Milstein,
628   *J. Am. Chem. Soc.*, 1998, **120**, 12539-12544.
629 13.   M. Albrecht, P. Dani, M. Lutz, A. L. Spek and G. van Koten, *J. Am. Chem. Soc.*, 2000,
630   **122**, 11822-11833.
631 14.   M. Kanzelberger, B. Singh, M. Czerw, K. Krogh-Jespersen and A. S. Goldman, *J. Am.
632   Chem. Soc.*, 2000, **122**, 11017-11018.
633 15.   R. A. Baber, R. B. Bedford, M. Betham, M. E. Blake, S. J. Coles, M. F. Haddow, M. B.
634   Hursthouse, A. G. Orpen, L. T. Pilarski, P. G. Pringle and R. L. Wingad, *Chem.
635   Commun.*, 2006, **0**, 3880-3882.
636 16.   D. F. MacLean, R. McDonald, M. J. Ferguson, A. J. Caddell and L. Turculet, *Chem.
637   Commun.*, 2008, **0**, 5146-5148.

638	17.	W. H. Bernskoetter, S. K. Hanson, S. K. Buzak, Z. Davis, P. S. White, R. Swartz, K. I.
639		Goldberg and M. Brookhart, *J. Am. Chem. Soc.*, 2009, **131**, 8603-8613.
640	18.	J. Meiners, A. Friedrich, E. Herdtweck and S. Schneider, *Organometallics*, 2009, **28**,
641		6331-6338.
642	19.	B.-S. Zhang, W. Wang, D.-D. Shao, X.-Q. Hao, J.-F. Gong and M.-P. Song,
643		*Organometallics*, 2010, **29**, 2579-2587.
644	20.	D. Milstein, *Topics in Catalysis*, 2010, **53**, 915-923.
645	21.	J.-L. Niu, X.-Q. Hao, J.-F. Gong and M.-P. Song, *Dalton Trans.*, 2011, **40**, 5135-5150.
646	22.	P. Majumder, S. Baksi, S. Halder, H. Tadesse, A. J. Blake, M. G. B. Drew and S.
647		Bhattacharya, *Dalton Trans.*, 2011, **40**, 5423-5425.
648	23.	N. Nebra, J. Lisena, N. Saffon, L. Maron, B. Martin-Vaca and D. Bourissou, *Dalton*
649		*Trans.*, 2011, **40**, 8912-8921.
650	24.	C. J. Moulton and B. L. Shaw, *J. Chem. Soc., Dalton Trans.*, 1976, 1020-1024.
651	25.	M. E. van der Boom and D. Milstein, *Chem. Rev.*, 2003, **103**, 1759-1792.
652	26.	J. T. Singleton, *Tetrahedron*, 2003, **59**, 1837-1857.
653	27.	J. Choi, A. H. R. MacArthur, M. Brookhart and A. S. Goldman, *Chem. Rev.*, 2011, **111**,
654		1761-1779.
655	28.	D. S. McGuinness, P. Wasserscheid, W. Keim, D. Morgan, J. T. Dixon, A. Bollmann,
656		H. Maumela, F. Hess and U. Englert, *J. Am. Chem. Soc.*, 2003, **125**, 5272-5273.
657	29.	S. P. Downing, M. J. Hanton, A. M. Z. Slawin and R. P. Tooze, *Organometallics*, 2009,
658		**28**, 2417-2422.
659	30.	B. Pitteri and M. Bortoluzzi, *Polyhedron*, 2008, **27**, 2259-2264.
660	31.	L. Canovese, G. Chessa, G. Marangoni, B. Pitteri, P. Uguagliati and F. Visentin, *Inorg.*
661		*Chim. Acta*, 1991, **186**, 79-86.
662	32.	C. Viñas, P. Anglès, G. Sánchez, N. Lucena, F. Teixidor, L. Escriche, J. Casabó, J. F.
663		Piniella, A. Alvarez-Larena, R. Kivekäs and R. Sillanpää, *Inorg. Chem.*, 1998, **37**, 701-
664		707.
665	33.	S.-Q. Bai, L. L. Koh and T. S. A. Hor, *Inorg. Chem.*, 2009, **48**, 1207-1213.
666	34.	M. Konrad, F. Meyer, K. Heinze and L. Zsolnai, *J. Chem. Soc., Dalton Trans.*, 1998,
667		199-206.
668	35.	F. Teixidor, L. Escriche, J. Casabo, E. Molins and C. Miravitlles, *Inorg. Chem.*, 1986,
669		**25**, 4060-4062.
670	36.	Y. Klerman, E. Ben-Ari, Y. Diskin-Posner, G. Leitus, L. J. W. Shimon, Y. Ben-David
671		and D. Milstein, *Dalton Trans.*, 2008, 3226-3234.
672	37.	F. Teixidor, G. Sanchez-Castello, N. Lucena, L. Escriche, R. Kivekas, M. Sundberg and
673		J. Casabo, *Inorg. Chem.*, 1991, **30**, 4931-4935.
674	38.	P. Braunstein and F. Naud, *Angew. Chem. Int. Ed.*, 2001, **40**, 680-699.
675	39.	M. Bassetti, A. Capone and M. Salamone, *Organometallics*, 2003, **23**, 247-252.
676	40.	B. S. Furniss, A. J. Hannaford, P. W. G. Smith and A. R. Tatchell, *Vogel's textbook of*
677		*practical organic chemistry*, 5th edn., J. Wiley and sons, New York, 1989.
678	41.	D. L. Reger, R. F. Semeniuc and M. D. Smith, *Cryst. Growth Des.*, 2005, **5**, 1181-1190.
679	42.	C. N. Temple, S. Gambarotta, I. Korobkov and R. Duchateau, *Organometallics*, 2007,
680		**26**, 4598-4603.
681	43.	S. G. M., *Acta Cryst., Sect. A:Fundam. Cryst.*, 2008, **64**, 112-122.
682	44.	A. L. Spek, *J. Appl. Cryst.*, 2003, **36**, 7-13.
683	45.	L. J. Farrugia, *J. Appl. Cryst.*, 1997, **30**, 565.
684	46.	R. J. C. Brown and R. F. C. Brown, *J. Chem. Educ.*, 2000, **77**, 724-731.
685	47.	T. C. O. Mac Leod, M. V. Kirillova, A. J. L. Pombeiro, M. A. Schiavon and M. D.
686		Assis, *Appl. Catal., A*, 2010, **372**, 191-198.

687 48. G. B. Shul'pin, G. Suss-Fink and L. S. Shul'pina, *J. Mol. Catal. A: Chem.*, 2001, **170**,
688   17-34.
689 49. M. V. Kirillova, A. M. Kirillov, D. Mandelli, W. A. Carvalho, A. J. L. Pombeiro and G.
690   B. Shul'pin, *J. Catal.*, 2010, **272**, 9-17.
691 50. S. Yiu, W. Man and T. Lau, *J. Am. Chem. Soc.*, 2008, **130**, 10821-10827.
692 51. M. V. Kirillova, Y. N. Kozlov, L. S. Shul'pina, O. Y. Lyakin, A. M. Kirillov, E. P.
693   Talsi, A. J. L. Pombeiro and G. B. Shul'pin, *J. Catal.*, 2009, **268**, 26-38.
694 52. L. S. Shul'pina, M. V. Kirillova, A. J. L. Pombeiro and G. B. Shul'pin, *Tetrahedron*
695   2009, **65**, 2424-2429.
696